Journal of Applied Polymer Science

A facile way to prepare two novel DOPO-containing liquid benzoxazines and their graphene oxide composites

Guomei Xu,[1,2] Tiejun Shi,[1] Quan Wang,[1] Jianhua Liu,[1] Yang Yi[1]

[1]School of Chemistry and Chemical Engineering of Hefei University of Technology, Hefei 230009, People's Republic of China
[2]School of Materials and Chemical Engineering of West Anhui University, Anhui, Lu'an 237012, People's Republic of China
Correspondence to: T. Shi (E-mail: stjhfut@163.com)

ABSTRACT: The design, preparation, and properties of two DOPO-containing compounds based on a cardanol-allylamine-paraformaldehyde benzoxazine (abbreviated as BZc-a) were described in this article. By controlling the amount of DOPO, it could react with BZc-a and generated different products. When DOPO: BZc-a <1 : 1, DOPO reacted only with allyl group, and generated a containing single DOPO group benzoxazine (P_1B); When DOPO: BZc-a ≧ 1 : 1, DOPO reacted not only with allyl group but also nucleophilic addition reaction, got a N-substituted derivative P_2B, which contain double DOPO groups. The chemical structure of P_1B and P_2B was characterized by ^{1}H-NMR and ^{13}C-NMR. Effect of DOPO on characteristics of BZc-a was investigated. Fire test demonstrated that P_1B and P_2B showed better flame retardance than BZc-a, and prepared two kinds of flame-retardance resin based on BZc-a. However, Field emission electron microscope observations showed the surface of P_1B and P_2B was very fragility, graphene oxide (GO) was chosen as to improve the surface performance. P_1B/GO-3 wt % and P_2B/GO-3 wt % composites were prepared by solution blending, and the thermal stability was studied by thermogravimetric analysis. © 2014 Wiley Periodicals, Inc. J. Appl. Polym. Sci. **2015**, *132*, 41634.

KEYWORDS: biomaterials; flame retardance; properties and characterization; resins; thermosets

Received 7 July 2014; accepted 12 October 2014
DOI: 10.1002/app.41634

INTRODUCTION

Benzoxazine (3,4-dihydro-3-substituted-2H-1, 3-benzoxazine) is typically synthesized by condensation of a phenol, formaldehyde, and an amine (aliphatic or aromatic) either by employing solution or solventless method.[1] It has been observed that benzoxazine's ring-opening polymerization occurred in the presence of heat or catalysts to formed a novel phenolic structures by a Mannich base bridge [-CH_2-N(R)-CH_2-], and the structure is similar to traditional phenolic resin network polymer.[2] As a result, this new kind of phenolic resin is also known as ring-opening polymerization phenolic resin.[3] The molecular structure of benzoxazine offers enormous design flexibility. General points out that benzoxazines have great potential application and research value, suitable for making high-performance materials.[4] Phthalonitrile-based prepolymers with low molecular weight show high thermal stability.[5] Brunovska designed a kind of benzoxazine monomer based on phthalonitrile, there phthalonitrile was intended to stabilize the Mannich bridge and to improve the thermal stability of polybenzoxazines; the results demonstrated that Phthalonitrile functional polybenzoxazines show high thermal stability, 5% weight loss (T_5) occurred at 450°C for monofunctional polybenzoxazines, polybenzoxazines from the bifunctional precursors even higher and up to 550°C.[6] Kim prepared a graphite composite based on polybenzoxazine with an imidazole (Im)-based catalyst; this graphite/polybenzoxazine composite could be successfully molded as a bipolar plate with excellent physicochemical properties through a compression molding process.[7]

With the deepening of the study, research on multifunction polybenzoxazines was attractive to many fields.[8] People started to look forward to synthesizing benzoxazine based on specific function, such as good thermal stability, flame retardant, and so on.[9] Various kinds of additive and reactive flame retardants containing phosphorus are increasingly potential for halogen-free to replace halogenated flame retardants for different polymeric materials and applications.[10] Phosphorus can work in the condensed phase by improving charring, yielding intumescences, or through inorganic glass formation; and in the gas phase through flame inhibition.[11] According to reported in the literature, occurrence and efficiency of flame retardance depend, not only on the flame retardant itself, but also on its interaction with pyrolyzing polymeric material and additives.[12] Flame retardancy can be attained through adding synergists/adjuvants, modification of the flame retardant,[13] and endow polymeric

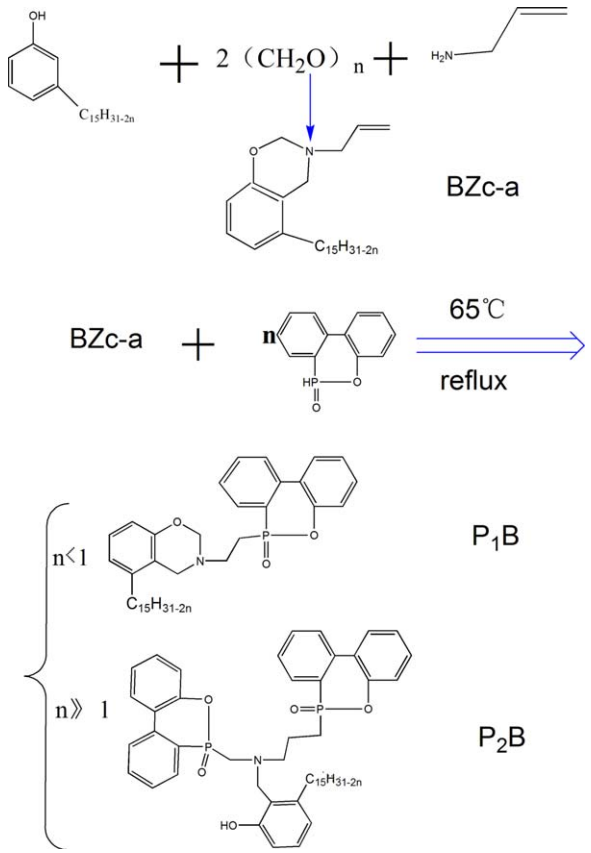

Scheme 1. Synthesis route of DOPO react with benzoxazine. [Color figure can be viewed in the online issue, which is available at wileyonlinelibrary.com.]

material with good flame retardance. DOPO was a new flame retardant intermediate. P-H bond in DOPO with high activity could take reaction with olefin, epoxy bonds and carbonyl, generated many available derivatives.[14] DOPO and its derivatives not only could be used as reactive and additive flame retardant, but also could be used in linear polyester, polyamide, epoxy resin, polyurethane, and other polymer flame retardant processed.[15] Lin prepared three aromatic diamine-based, phosphinated benzoxazines from three typical aromatic diamines-4,4′-diamino diphenyl methane,[16] 4,4′-diamino diphenylsulfone, and 4,4′-diamino diphenyl ether by a one-pot procedure. The results demonstrated that these materials offered high thermal stability and good flame retardancy.[17]

The main objective of this study was to prepare two novel DOPO-containing resins flame retardant, which were synthesized based on a liquid benzoxazine. A liquid benzoxazine monomer (BZc-a) prepared from cardanol,[18] allylamine, and paraformaldehyde. P-H bond in DOPO with high activity could take reaction with olefin, so it could react with benzoxazine (BZc-a) which contain allyl group and generated different compounds. When DOPO: BZc-a <1 : 1, DOPO reacted only with allyl group, and a benzoxazine contained one DOPO group (P_1B) generated. The content of phosphorus was 7.7%; when DOPO: BZc-a ≧ 1 : 1, DOPO reacted not only with allyl group but also nucleophilic addition reaction, got a N-substituted P_2B, which contain two DOPO groups, its content of phosphorus up to 9.8%. P_1B and P_2B had similar chemical structure could be used as two new kinds of flame retardant and to improve the flame retardance in resin. The properties of P_1B and P_2B were characterized by ^{1}H-NMR and ^{13}C-NMR. Fire test demonstrated that P_1B and P_2B showed better flame retardance than BZc-a, turned BZc-a from flammable to a noncombustible material. However, from the images of FESEM, the surface of P_1B and P_2B were very fragility, as to improve the flexibility of P_1B and P_2B, then graphene oxide (GO) made in our laboratory was added in them and got P_1B/GO-3 wt % and P_2B/GO-3 wt % composites. The properties of these composites were studied in this article and the thermal stability was studied by TGA. The FESEM images of composites demonstrated that the tenacity of these materials enhanced greatly after blended with GO.

EXPERIMENTAL

Materials

Cardanol (90%) was purchased from Shangdong Haobo Biological Material Co., Ltd. $M = 304.52$; Graphite powder was kindly supplied by Hefei General Machinery Research Institute, the average size of which is 75 μm; DOPO, alcohol, and paraformaldehyde was purchased from Shanghai Chemical Reagents Company and used as received; allylamine (85%) was bought from Tianjin chemical reagent factory.

Benzoxazine (BZc-a) was made in our laboratory by Mannich reaction of cardanol, paraformaldehyde, and allylamine; the chemical structure of BZc-a was shown in Scheme 1 and the other properties were shown in elsewhere.[19] All the reagents used throughout this study were used "as is" without any further purification. Deionized water was used in the whole work.

Preparation of P_1B and P_2B

One pot synthesis was used to preparation of P_1B and P_2B.

Synthesis of P_1B: 24.36 g (0.05 mol) BZc-a and 5.5 g (0.025 mol) DOPO were placed in a 500 mL three-neck round flask equipped with magnetic stirrer, thermometer, reflux condenser, and 200 mL alcohol. The reaction continued for 8 h at 65°C in nitrogen atmosphere, the crude of the reaction removed alcohol under vacuum. About 20.12 g products were obtained by purification on silica gel column; the solvent used for silica gel column was a mixed solvent which was 5% alcohol, 30% petroleum ether, and 65% dichloromethane. The synthesized route was shown in Scheme 1. A maroon sticky liquid product was isolated.

Synthesis of P_2B: 24 g (0.05 mol) BZc-a and 24 g (0.11 mol) DOPO were mixed in a 500 mL three-neck round flask. The specific route of synthesis was described as above, and was shown in Scheme 1. About 35.32 g maroon sticky liquid product was obtained. The product was purified through silica gel column; the solvent used for silica gel column was a mixed solvent which was 10% alcohol, 20% petroleum ether, and 70% dichloromethane.

Preparation of GO

The oxidized graphite was synthesized from expanded graphite power in our laboratory via improved Hummer's method,[20]

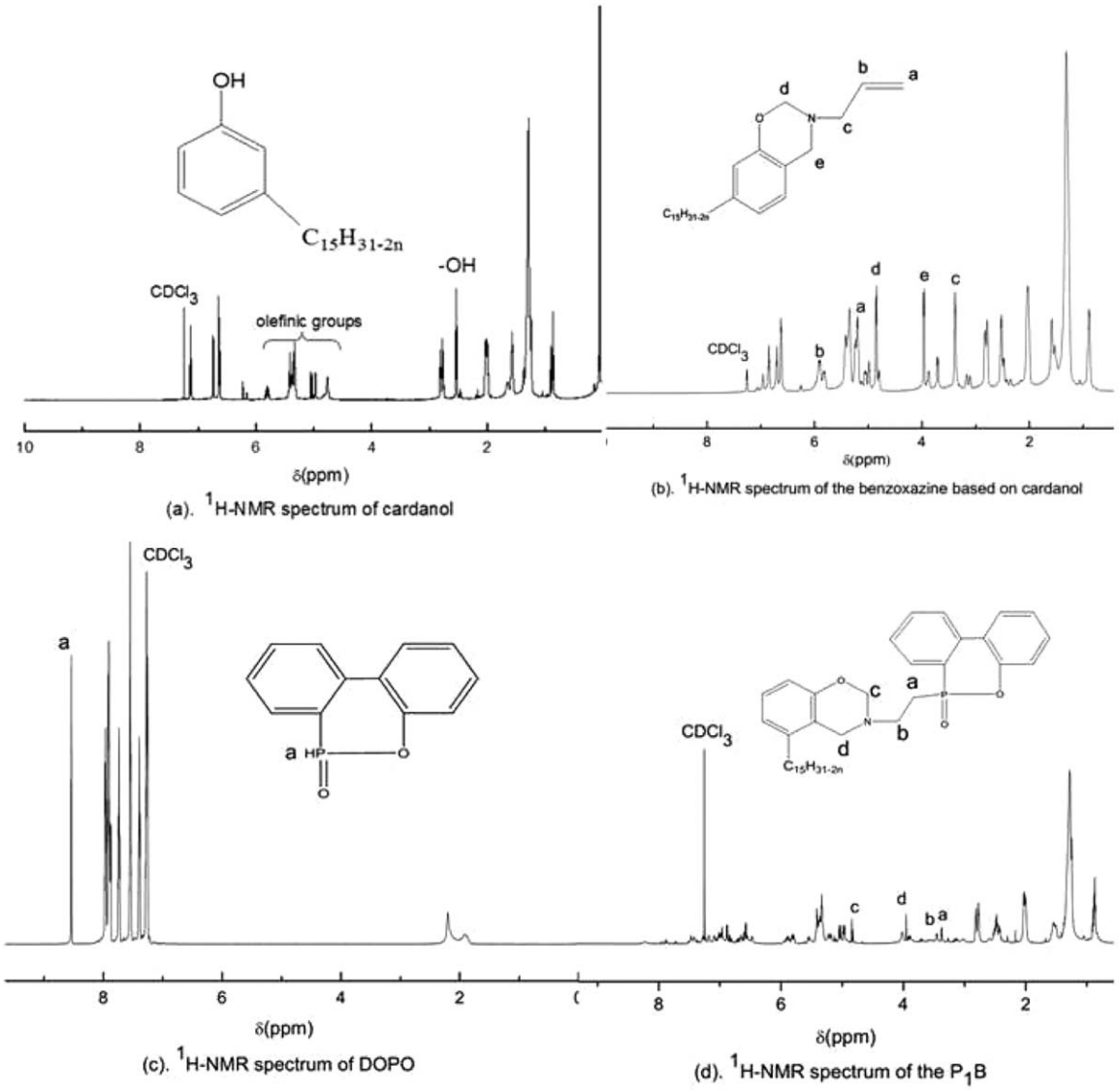

Figure 1. ^{1}H-NMR spectrum of P_1B.

concentrated sulfuric acid (360 mL) and concentrated phosphoric acid (40 mL) were added to a mixture of graphite powder (3 g) and potassium permanganate (12 g), stirred for 10 min, then heated to 50°C, and continued stirred for 12 h. The reaction was stopped by ice bath then 30% H_2O_2 was added. The mixture was washed with water to neutral. About 30% hydrochloric acid was added into the obtained solid, and continued washed with water and filtered till to neutral. Then, GO was obtained by the ultrasonication and centrifugation of the unoxidized graphite. GO was used throughout this study without any further work.

Preparation of BZc-a/GO and PB/GO Blends

BZc-a/GO and PB/GO mixtures were prepared in alcohol by solution blending.[21] Combined 5 g BZc-a, 5 g P_1B, and 5 g P_2B with 3 wt % GO (0.15 g) at elevated temperature in 100 mL alcohol, respectively. The mixtures followed by stirring at 80°C for 2 h and then were placed in a vacuum oven at 60°C for 2 days to remove alcohol.

Thermal Curing of the Benzoxazine Precursors and its Mixtures

BZc-a, P_1B, P_2B, BZc-a/GO, P_1B/GO, and P_2B/GO were all heated in a stainless rectangular mold with a stepwise cure in an air-circulating oven. The step profile for curing was as follows: 100°C for 2 h, 120°C for 2 h, 140°C for 2 h, 180°C for 2 h, 200°C for 2 h. It was noted that P_2B/GO cured completely when temperature elevated to 180°C for 2 h, and BZc-a was not completely cured when temperature elevated to 200°C for 2 h, and added one curing procedure at 240°C for 1 h.

Measurements

Field emission electron microscope (FE-SEM) observations were conducted on a FEI Sirion SU8020 system with an accelerating voltage of 1 kV. FTIR spectra were collected in transmission mode on spectrophotometer (Thermo Nicole, Nicolele-6700) with KBr as reference. Thermogravimetric analysis (TGA) was conducted on TGA Q5000 (New Castle, DE) at a heating rate of 10°C/min in nitrogen atmosphere. The gas flow rate was

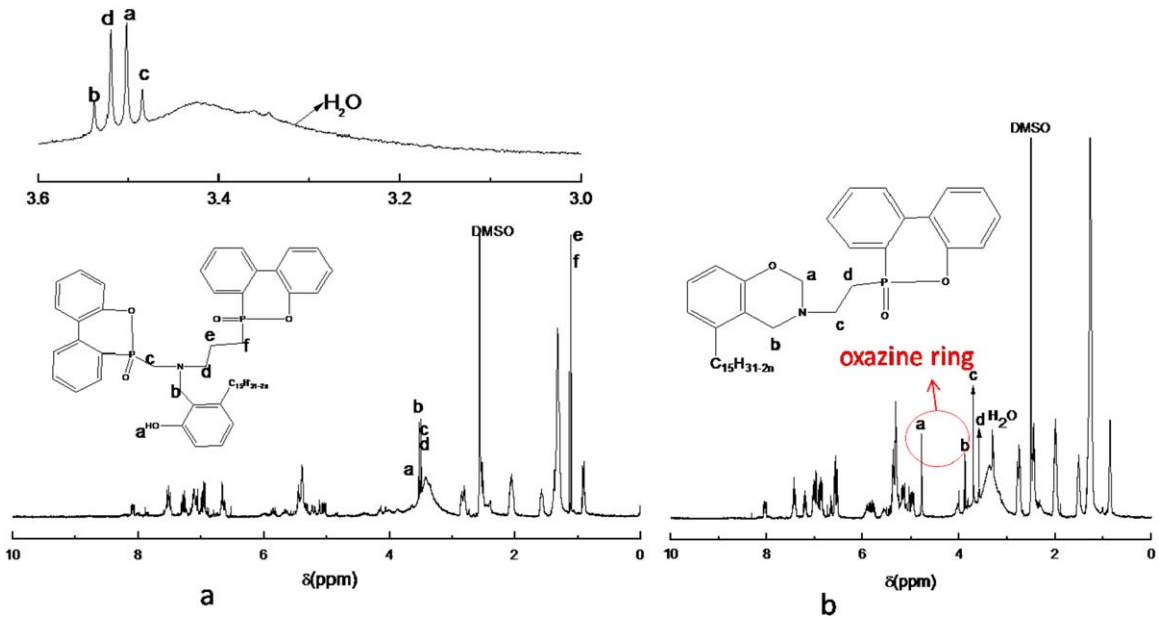

Figure 2. ^{1}H-NMR spectrum of P_2B. [Color figure can be viewed in the online issue, which is available at wileyonlinelibrary.com.]

100 mL/min. ^{1}H-NMR spectra were recorded in DMSO-d6 and $CDCl_3$ on an AVANCE III 400 instrument of 400 MHz (Brooke, Swiss), ^{13}C-NMR spectra were recorded in DMSO-d_6 on a VNMRS600 instrument of 600 MHz (Agilent, America). Water bath ultrasonication was performed with a KQ-100E sonicater (100 W). TEM images were taken on a Hitachi SU8020 TEM at an accelerating voltage of 200 kV by depositing specimen aqueous solution onto copper grids.

The burning behavior by limited oxygen index was performed according to GB/T 2406 with a test specimen bar of 95 mm in length, 7 mm in width and about 2.8 mm in thickness, which was performed on a XZT-100A (ChengDe Testing Machine, China) apparatus for Limited Oxygen Index Testing. Each compound was prepared with two test specimen. By adjusting the proportion of nitrogen and oxygen in vertical glass bottle, the flame retardant experiment was performed.

RESULTS AND DISCUSSION

Characterizations of P_1B

Figure 1 shows the results of ^{1}H-NMR spectrum, these ^{1}H-NMR spectrum were all performed in $CDCl_3$, and the chemical shift was calibrated by setting the chemical shift of $CDCl_3$ as 7.26 ppm. To confirm the characterization of P_1B, the ^{1}H-NMR spectrum of cardanol, benzoxazine based on cardanol and DOPO are also presented. So there are four figures in the Figure 1. The ^{1}H-NMR spectrum of cardanol is shown in the Figure 1(a); the peak at 2.54 ppm is the phenolic protons of –OH (a). As reported in the literature, there would be two or three olefin groups in the cardanol's long side chain, which are confirmed in the Figure 1(a), for there are four multipeaks among 4.75–5.80 ppm belongs to double bonds. The ^{1}H-NMR spectrum changed when cardanol was used to synthesized benzoxazine, which is shown in the Figure 1 (b). Compare Figure 1(a) and 1(b), the characteristic protons of oxazine ring appeared; the two peaks at 3.98 and 4.82 ppm are assigned to–Ar–CH_2–N– (e) and –O–CH_2–N–(d), respectively, which are not be found in the ^{1}H-NMR spectrum of cardanol. The two resonances at 5.20 and 5.90 ppm are typical for protons of CH_2 (a) and CH–(b) in the vinyl group, respectively. The peak at 3.37 ppm would be assigned to the protons (c) located between the vinyl group and the nitrogen atom.[22] In addition, the resonances at 6.25−6.9 ppm are assigned to the protons of the aromatic ring; the protons of aliphatic group in the cardanol's side chain are observed around 0.89–2.81 ppm, which as same as shown in Figure 1(a). The Figure 1(c) shows the characteristic protons of DOPO. By controlling the amount of DOPO and benzoxazine, P-H bond in DOPO first take reaction with allyl group and generated P_1B. The chemical structure of P_1B is shown in the Figure 1(d); there appeared not only the properties of benzoxazine but also that of DOPO.[23] The oxazine ring still exist and appear at 3.95 (d) and 4.85 (c) ppm, which also be found in the ^{1}H-NMR spectrum of benzoxazine. The resonance at 5.20 ppm assigned to the proton of CH– in the vinyl group disappeared, appeared the two peaks at 3.36 and 3.45 ppm assigned to the protons (a, b) of CH_2 located between the -P=O and N. In addition, the resonances at 8.54 ppm assigned to the protons of P-H in DOPO were also disappeared and appeared many multipeaks among 6.46−7.87 ppm were assigned to the protons of the aromatic rings, the protons of aliphatic group in the cardanol's side chain were observed around 0.87–2.82 ppm. It is important to note that there are four multipeaks among 4.75–5.80 ppm belongs to the characteristic of olefinic groups in the side chain of cardanol still existed in the ^{1}H-NMR spectrum of P_1B, which is helpful to determine the reaction occurred only between the allyl group and DOPO. All these data could support P_1B was prepared successfully.[24]

Characterizations of P_2B

In this work, we take advantage of the nucleophilicity of DOPO and the ring-opening characteristic of benzoxazines to prepare

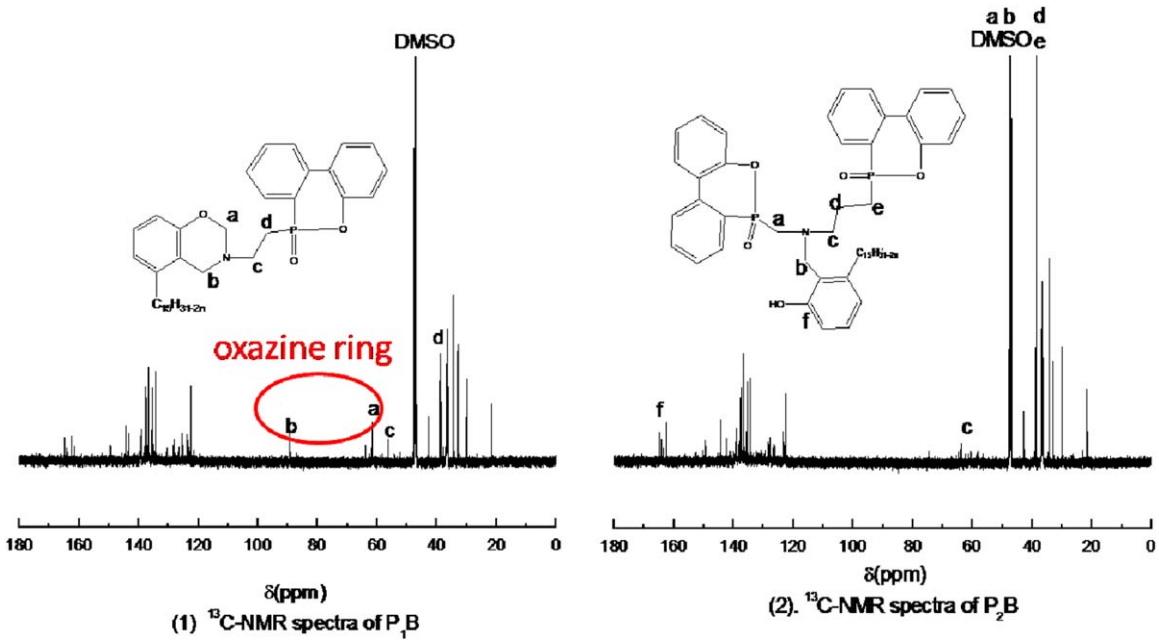

Figure 3. ^{13}C-NMR spectrum of P_1B and P_2B. [Color figure can be viewed in the online issue, which is available at wileyonlinelibrary.com.]

phenol with two phosphinate pendants. Therefore, P_2B were prepared via the nucleophilic addition of DOPO on benzoxazine. To confirm the chemical structure of P_2B, ^{1}H-NMR spectra were recorded in DMSO-d_6 on a VNMRS600 instrument of 600 MHz (Agilent, America). To verify the phenolic OH was really generated via the ring-opening of benzoxazine, we also performed the ^{1}H-NMR spectrum of P_1B in DMSO-d_6 on the same instrument. The ^{1}H-NMR spectrum results are shown in Figure 2.

Figure 2(a) shows the ^{1}H-NMR spectra of P_2B. By comparing the ^{1}H-NMR spectra of P_1B and P_2B, it could be clearly seen that the characteristic oxazine peaks of P_1B at 4.78 (a) and 3.89 ppm (b) disappeared in P_2B, while three methylene signals of (b) at 3.53, (d) 3.52, and (c) 3.48 ppm appeared. It is noteworthy that a signal at 3.50 ppm representing the phenolic OH (a) was observed in P_2B. Apart from these, two methylene signals of P_2B at 1.13 ppm (e) and 1.08 ppm (f) also appeared. All these spectroscopic data supported the ring opening of oxazine and generated the phenolic OH in P_2B. The signals of each protons of the aromatic ring of P_1B are also existed in P_2B; however, the intensity of these peaks became strong. In addition, the protons of aliphatic group in the cardanol's side chain are observed around 0.89–2.85 ppm.

Figure 3 shows the ^{13}C-NMR spectra of P_1B and P_2B. By comparing the ^{13}C-NMR spectra of P_1B and P_2B, it could be seen that the characteristic oxazine ring peaks of P_1B at 61.56 (Ca) and 89.28 ppm (Cb) disappeared in P_2B, while five methylene signals at 47.9 (Ca) and 47.8 (Cb) and 56.16 ppm (Cc) and 39 ppm (Cd, Ce) appeared. The same spectroscopic information is also present in the ^{1}H-NMR spectra of P_1B and P_2B, which supported the ring opening of P_1B, and obtained P_2B. Besides, the signal at 164.8 ppm (Cf) supported the Ar–OH structure. The carbons of aliphatic group in the cardanol's side chain are also observed around 22.2–42.8 ppm. All these are helpful us to understand the structures of P_1B and P_2B.

Characterizations of GO

The FTIR spectra of oxidized graphite and expanded graphite are shown in Figure 4. The adsorption bands corresponding to the C=O carbonyl stretching at 1730 cm^{-1}, the O-H deformation vibration at 1390 cm^{-1}, and the C–O stretching at 1226 and 1062 cm^{-1}, which are all identified in the FTIR spectra of oxidized graphite. Besides the ubiquitous O-H stretches, which appear at 3403 cm^{-1} as a broad and intense signal, the resonance at 1623 cm^{-1} can be assigned to the vibrations of unoxidized C=C bonds in expanded graphite. All these confirmed

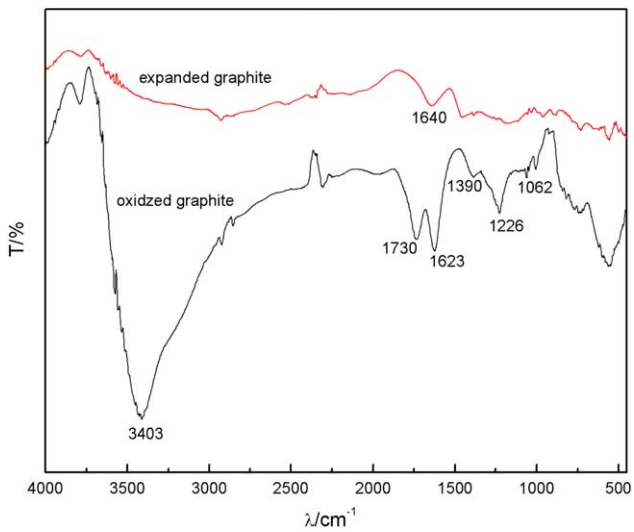

Figure 4. FTIR spectra of oxidized graphite and expanded graphite. [Color figure can be viewed in the online issue, which is available at wileyonlinelibrary.com.]

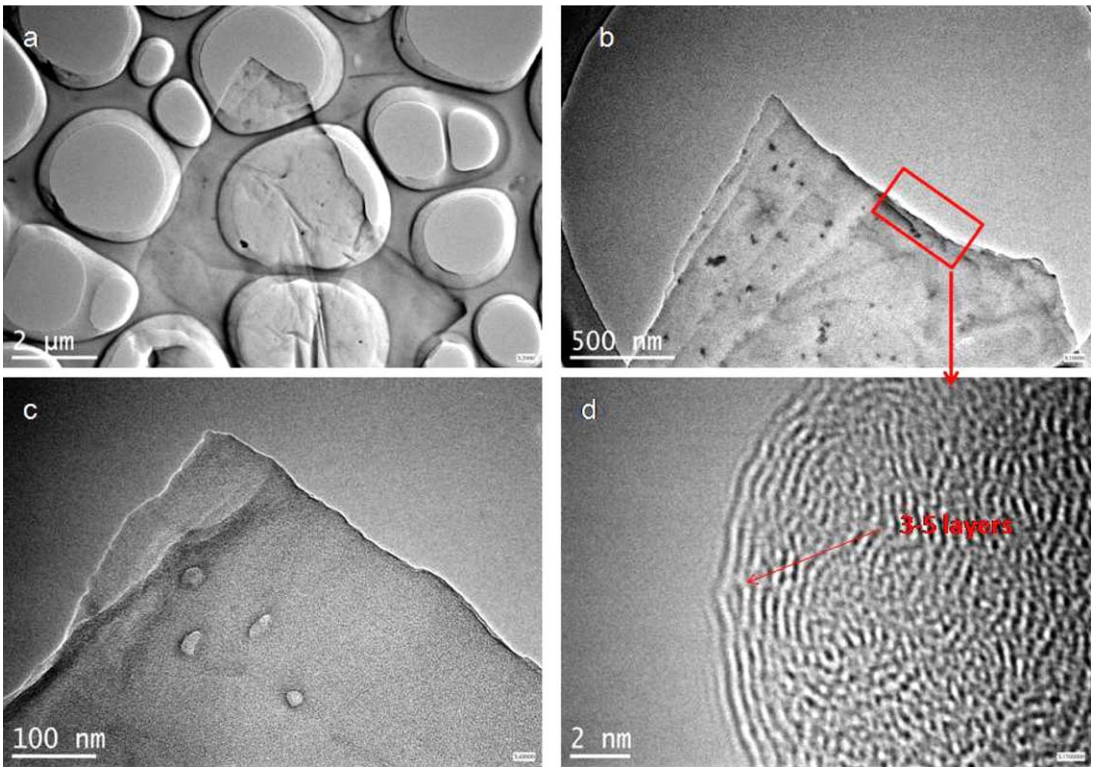

Figure 5. TEM images of GO dispersed in alcohol (a–d). [Color figure can be viewed in the online issue, which is available at wileyonlinelibrary.com.]

that the graphite was oxidized and oxygen containing groups were introduced onto the oxidized graphite.[25]

Following that, GO was obtained via ultrasonication and centrifugation of the unoxidized graphite. To verify GO was successfully prepared from oxidized graphite. The morphologies of GO were observed directly by transmission electron microscopy (TEM). The sample was taken on a Hitachi SU8020 instrument at an accelerating voltage of 200 kV by depositing exfoliated GO on a copper mesh form an alcohol aqueous dispersion.[26]

The morphologies of multiple dimensions of GO are shown in Figure 5. It is clearly visible that thin sections attached on the copper in Figure 5(a) and large particles are not detected. Figure 5(a) showed GO sheets are nearly transparent and curled at the edges. Figure 5(b,c) shows the edges of the suspended film always fold back, allowing for a cross-sectional view of the film, single GO sheets together with ultrathin stacks of GO sheets were obtained which demonstrated that graphite oxide had been effectively exfoliated and uniformly dispersed in the alcohol matrix. The observation of these edges by high-resolution TEM provides the GO sheets were effectively exfoliated to be three to five layers which were shown in Figure 5(d). All these results proved the successful oxidation of graphite to graphite oxide in our laboratory.

Preparation and Characterization of BZc-a/GO and PB/GO Blends

We found something interesting, that was, GO could not stabilize the dispersion in BZc-a; however, it could stay stable in P_1B and P_2B, when 3 wt % GO blended with BZc-a, P_1B, and P_2B, respectively. Figure 6 shows the morphologies of GO dispersed in these composites. The first sample is GO dispersed in BZc-a alcohol solution, GO had deposited at the bottom of tube; the second and the third sample all show a homogeneous solution. These data suggested that P_1B-GO and P_2B-GO hybrid product generated, which enhanced the interfacial interaction of GO with PB matrix.

A detailed understanding facilitates GO dispersion; TEM is employed since it could provide better qualitative understanding of the internal structure, spatial distribution, and dispersion of

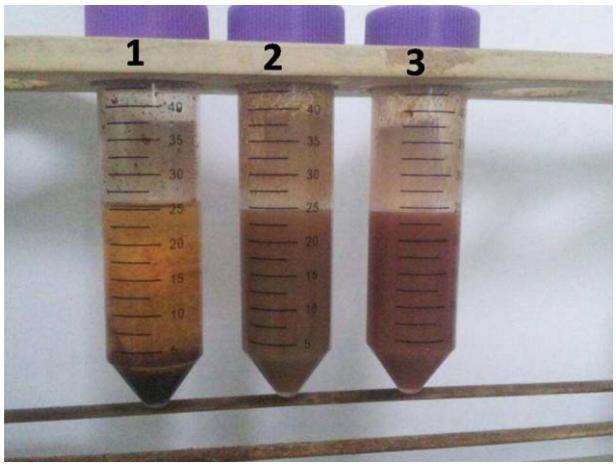

Figure 6. Digital photos of GO dispersed in the BZc-a/GO (1), P_1B/GO (2), and P_2B/GO (3) mixtures. [Color figure can be viewed in the online issue, which is available at wileyonlinelibrary.com.]

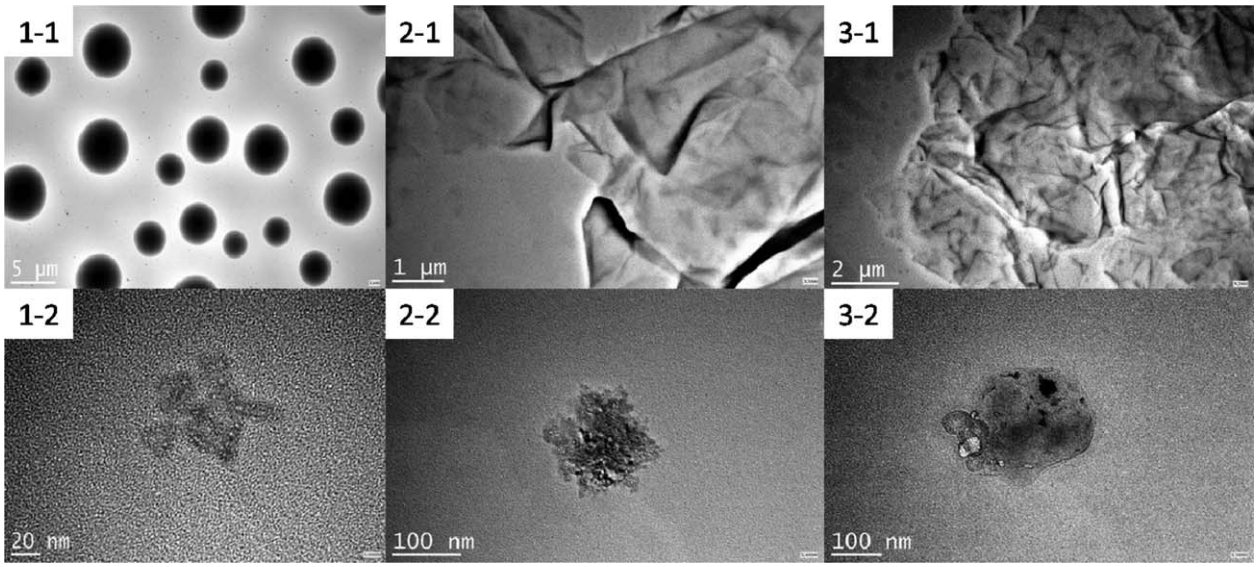

Figure 7. TEM images of GO dispersed in BZc-a (1), P_1B (2), and P_2B (3) matrix.

GO sheets through direct visualization. TEM images of GO dispersed in those mixtures are shown in Figure 7.

As shown in Figure 7, these TEM images typical of 3 wt % GO mixed with BZc-a, P_1B, and P_2B are rather different from that of GO (Figure 5). The top images of Figure 7 are the whole profile of these mixtures deposited on copper mesh. As shown in Figure 7 (1-1) there is almost nothing existed, just many bubbles, which demonstrated that GO would not dispersed in BZc-a and agreement with Figure 6. BZc-a was synthesized with cardanol, which is a by-product of cashew nut contain many other grease properties.[27] The oil characteristics of cardanol prevented the good deposition of BZc-a onto copper grids. As shown in Figure 7 (2-1, 3-1), it could be seen that thin sections attached on the copper grids and no large agglomerates observed. Following that we observed through high magnification, the images are shown at the bottom of Figure 7. Wherein the GO sheets are represented as the black sheet, and the BZc-a, P_1B, P_2B matrix are represented as the gray background, respectively. As shown in the Figure 7 (2-2, 3-2), a small amount of GO sheets are observed at high magnification (×40,000) dispersed as tactoids with several stacked layers and most of the sheets are exfoliated into individual layers and, in the Figure 7 (1–2), there is a fuzzy image of GO sheets dispersion, which could be explained by the surfaces of GO sheets were highly oxygenated, bearing hydroxyl, epoxide, diol, ketone, and carboxyl functional groups that could be reaction with P_1B and P_2B, and generated P_1B-GO and P_2B-GO hybrid, which affects the compatibility between the GO sheets and the P_1B, P_2B matrix. Therefore, GO dispersed better in P_1B, P_2B matrix than in BZc-a.

The homogeneous dispersion of GO in P_1B and P_2B matrix suggested that P_1B-GO and P_2B-GO hybrid product generated, which enhanced the interfacial interaction of GO with PB matrix. The possible mechanism of P_2B-GO was chosen as a representative and addressed in Scheme 2. The FTIR spectra of P_2B and P_2B/GO blends are all shown as to confirm the mechanism.

The chemical structure of P_2B and P_2B/GO-3 wt % blends had been characterized with FTIR. The results are shown in Figure 8. The phosphoryl stretching vibration was one of the most useful indications in the vibrational spectrum of organophosphorus compounds, and had extensive study. In the FTIR spectrum of P_2B, there are good correlations for the P-O-C (phenyl) at 1204 cm^{-1} and P-O-C (alkyl) was in the range of 1050–995 cm^{-1}. The absorption peaks of -OH at 3403 cm^{-1}, all these results demonstrated the structure of P_2B. When P_2B mixed with 3 wt % GO, they had made hybridization, and prepared P_2B/GO blends. The absorption of the -OH group in P_2B at

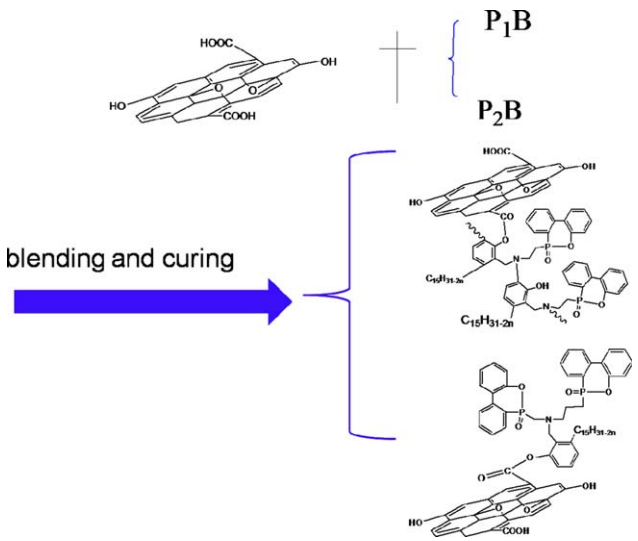

Scheme 2. Synthesis route of P_1B and P_2B blended with GO. [Color figure can be viewed in the online issue, which is available at wileyonlinelibrary.com.]

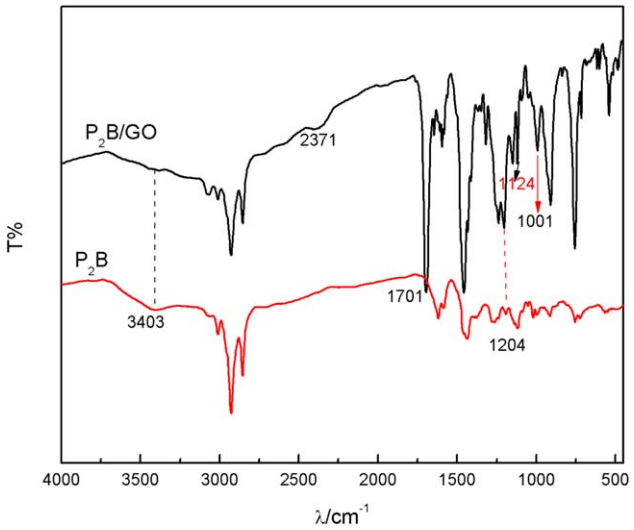

Figure 8. FTIR spectra of P_2B and P_2B/GO-3 wt % composite. [Color figure can be viewed in the online issue, which is available at wileyonlinelibrary.com.]

3403 cm^{-1} disappeared and appeared a strong absorption at 1701 cm^{-1}, which was the characterized absorption of -O-C=O- group. In the FTIR spectrum of P_2B/GO mixture, there were also much characteristic absorptions for the P-O-C (phenyl) at 1204 cm^{-1} and C-O stretching vibrations were shown at 1124 cm^{-1} and a sharp band at 1001 cm^{-1}.

Differential scanning calorimetry (DSC) is an important tool to observe the curing behavior because it can provide detailed knowledge of the cure mechanism and the preferred cure temperature during the formation of three-dimensional networks in materials.[28] In this study, DSC has been employed to elucidate the curing behavior of these samples; and the result is shown in Figure 9. There are two figures in Figure 9, the left of which is the DSC curve of BZc-a, P_1B and P_2B; the right of which is the DSC curve of these samples mixed with 3 wt % GO. The baselines in these DSC curves are not flat and irregular which would be BZc-a, P_1B and P_2B are not high purity; when these samples blended with GO resulting the curing peaks difficult to observe due to there are too moieties in samples. The DSC curve of BZc-a is much different from that of BZc-a reacted with different amount of DOPO. There exists a strong exothermal peak around 240°C during BZc-a curing in N_2 atmosphere. However, there is a weak exothermal peak at 230°C in P_1B and scarcely any exothermic peaks existed during P_2B curing, and all appeared one endothermic peak at 140 and 130°C, respectively. Exothermic reaction would corresponded to an oxazine ring existed in P_1B, and no oxazine ring present in P_2B; and endothermic reaction which corresponded to the fracture of -P=O group or remaining DOPO absorption heat caused. The DSC curves are not going to change too much after all these samples mixed with 3 wt % GO. The DSC curve of BZc-a/GO just slightly shifted the exothermal peak to a higher temperature at 242°C. However, during the cure process of P_1B/GO, there are two peaks, the first is a endothermic peak at 132°C, which corresponded to the fracture of -P=O group[29]; the second is a unconspicuous exothermic peak at 170°C, which corresponded to the opening of oxazine ring. The exothermic peak of P_1B/GO shifted to a much lower temperature than that of BZc-a/GO, which was due to the fact that oxazine ring opening need acidic initiator. P_1B is a substance contains oxazine ring and DOPO. As P_1B blended with 3 wt % GO, hydroxyl, epoxide, diol, ketone, and carboxyl functional groups contained in GO catalyzed the polymerization.[30] Meanwhile, no exothermic peak appeared during the curing process of P_2B/GO, just appeared a broad endothermic peak at 125°C, which would be due to the fact that there is no oxazine ring exist in P_2B, only two –P=O groups, so the curing behavior different from that of each other.

Performance and Characterization of BZc-a/GO After Cured and PB/GO Composites

Flame Retardancy. As everyone knows DOPO-based compound show a high propensity to achieve efficient flame inhibition, since the DOPO structure acts as a precursor for the release of PO during pyrolysis.[31] In this article, P_1B and P_2B is a kind of contain phosphorus compounds. So P_1B and P_2B would also

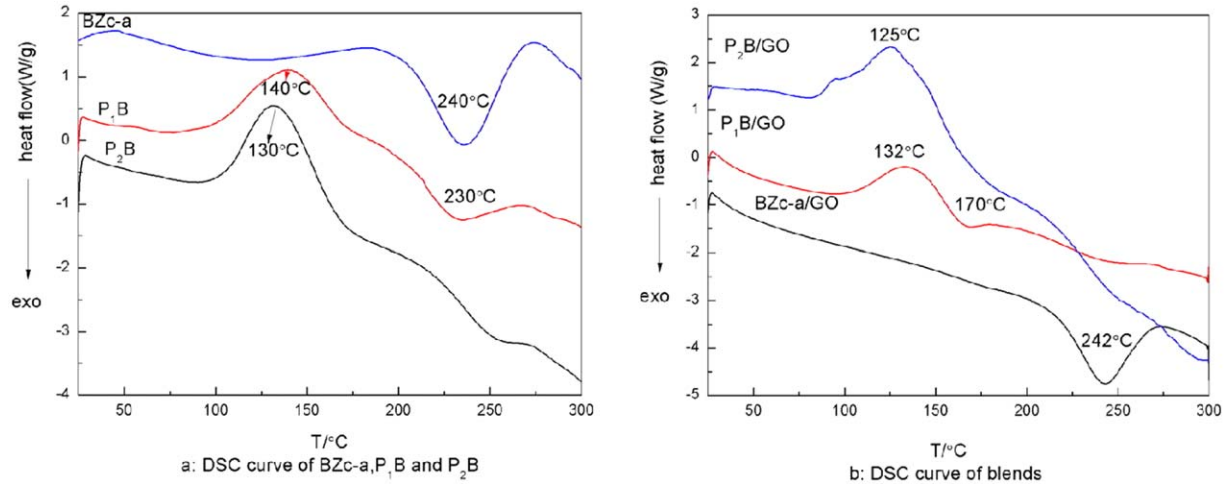

Figure 9. DSC analysis. [Color figure can be viewed in the online issue, which is available at wileyonlinelibrary.com.]

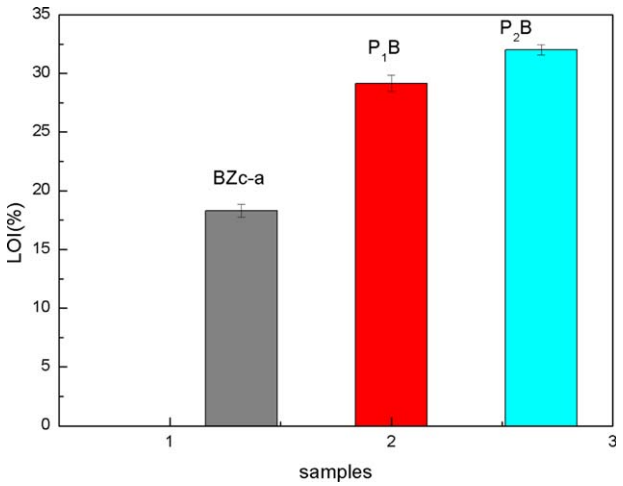

Figure 10. The burning behavior by oxygen index of BZc-a and P_1B and P_2B after cured. [Color figure can be viewed in the online issue, which is available at wileyonlinelibrary.com.]

have certain flame retardant performance. The burning behavior by limited oxygen index of BZc-a and P_1B and P_2B after cured were carried out according to GB/T 2406 with a test specimen bar of 95 mm in length, 7 mm in width, and about 2.8 mm in thickness. In the test, each material prepared with two test specimen bars, the results are shown in Figure 10. The polybenzoxazine could burn in air and LOI was 18.3, which belong to a kind of flammable materials. However, when DOPO was introduced to BZc-a, the flame properties changed greatly. P_1B and P_2B they all could not burn in air, and LOI increased to 28 and 32, respectively, belong to a kind of noncombustible material.[32] This result show the better flame retardancy of P_1B and P_2B than BZc-a, which occurrence and efficiency depended, not only on the flame retardant DOPO itself, but also on its interaction with pyrolyzing polybenzoxazine.[33]

Thermal Analysis. The thermal stability of P_1B, P_2B, GO, BZc-a, and their mixtures were also analyzed by TGA after cured,[34] and the results are shown in Figure 11. Data related to the temperature corresponding to 5 wt % (T_5) and 10 wt % (T_{10}) weight loss of the initial weight, as well as residues at 800°C are summarized in Table I. In the figure, they all showed one decomposing stage except GO. GO displayed decompose during the whole process; however, the degradation rate of GO was slower than all other samples even when the temperature increased to 800°C, there were 76.4% residue. This would be attributed to the thermal exfoliation, degradation of oxide functionality groups. As seen from the TGA trace and Table I, the thermal properties of BZc-a changed when DOPO attached on it; basically, the most interesting aspect of this thermal analysis is the significant change of the char yield. The mass residue of BZc-a just was 1.13% at first, and that of P_1B and P_2B increased to 8.8 and 11.8%, increased by 7.7 and 10.7%, respectively. Significant differences in mass residue suggested that reduction of the BZc-a's flammability and implied good thermal stability. BZc-a was synthesized by cardanol; cardanol has a long aliphatic hydrocarbons side chain, which endowed BZc-a could burn easily, so the char yield of polybenzoxazine was very small. By incorporating different amount of DOPO, not only the potential of DOPO structure for phosphorus released then worked in the gas phase but also chemical reactions with BZc-a and DOPO, and their decomposition products might react into volatile or solid products depending on the chemical surroundings in the pyrolysis zone. However, there is another mechanism for the P_1B and P_2B flame inhibition, which is flame inhibition leads to a less complete combustion in the flame zone and resulted. Moreover, when BZc-a, P_1B, and P_2B blended with 3 wt % GO, the char yield increased to 11.5, 15.7, and 19.3%, respectively. In addition, the max decomposition temperature T_{max} also improved. There are two reasons for the thermal properties became better. The first would be due to the thermal degradation of GO proceeded by releasing noticeable amounts of CO_2 that could dilute the volatile flammable compounds and steal heat from the decomposition reaction so lowered the surface temperature of the composites. The second is might hydroxyl, epoxide, diol, ketone, and carboxyl functional groups on the surface of GO reacted with BZc-a, P_1B, and P_2B.

Characterizations of BZc-a/GO and PB/GO Composites by XRD and FESEM. The dispersion state of GO in composites is studied by XRD, which is an effective means to observe the exfoliation of GO in the composites. Figure 12 shows the XRD spectra of BZc-a/GO, P_1B/GO, and P_2B/GO composites after curing. The XRD spectra of graphite power and GO are shown on the top of Figure 12, Graphite exhibited a typical sharp (002) peak at 26.5° with a d-spacing of 0.336 nm. As GO was synthesized by graphite, GO showed a characteristic peak at 10.2°, with a corresponding d-spacing of 0.87 nm, attributed to the interlayer space between typical GO sheets needed to accommodate the water molecules trapped between oxygen-containing functional groups on GO sheets. When GO was incorporated into the P_1B, P_2B, BZc-a matrix, the XRD patterns of composites with contents of 3 wt % GO are almost the same as each other. They all show a broad peak at around 20.5°, which different from that of the raw material graphite, and not the characteristic diffraction peak of GO. Revealing that their

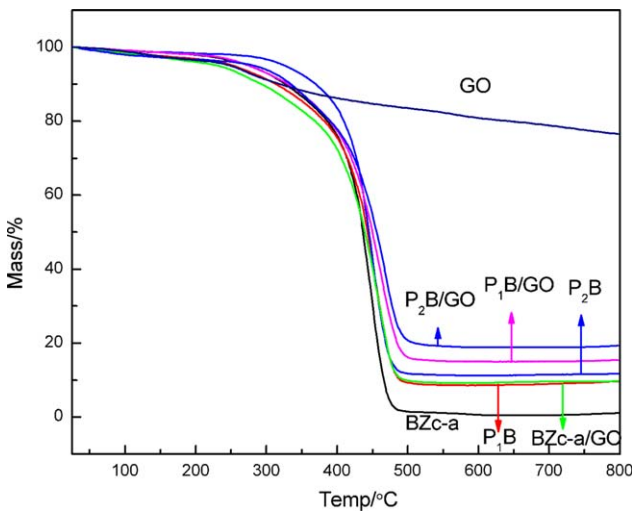

Figure 11. TGA trace of P_1B, P_1B/GO-3 wt %, P_2B, P_2B/GO-3 wt %, and BZc-a, BZc-a/GO-3 wt % after cured. [Color figure can be viewed in the online issue, which is available at wileyonlinelibrary.com.]

Table I. Decomposition Temperatures of Polybenzoxazine and the Composites

Sample	T_{max} (°C)	T_5 (°C)	T_{10} (°C)	Char yield (%) at 800°C
BZc-a	444	275	327	1.13
GO	455	249	320	76.4
P_1B	453	254	314	8.8
P_2B	452	264	370	11.8
P_1B/GO-3 wt %	466	276	331	15.7
P_2B/GO-3 wt %	474	247	335	19.3
BZc-a/GO-3 wt %	457	232	293	11.5

amorphous nature. The peak at 20.5° is slightly lower than that of raw graphite and is a broad diffraction peak, implying that BZc-a/GO, P_1B/GO, and P_2B/GO were composed of randomly ordered GO sheets with a corrugated structure.[35]

The cured samples are fractured and gold-coated in a FE-SEM observations were conducted on a SU 8020 system with an accelerating voltage of 1 kV for the observation of the cross section of the samples. The results are shown in Figure 13.

The surface morphologies of cured samples are observed by FESEM with different magnification scales. The surface of P_1B and P_2B is very brittle, which similar to the surface of glass. According to data in this article, adding DOPO could improve the flame retardancy of BZc-a, but also leaded to more brittle. As a consequence to improve the flexibility of P_1B and P_2B, P_1B/GO-3 wt % and P_2B/GO-3 wt % mixtures were made. The FESEM images afford important information of the dispersion of GO in P_1B and P_2B polymer matrix. The cross sections of cured mixtures are observed with different magnification scales. By compared, it could clear be seen the surface of these cured composites unlike P_1B and P_2B, exhibited a rough surface and appeared a large number of irregular wrinkles on the surface, which demonstrated that GO with flake or bundle structures were dispersed in P_1B and P_2B polymer matrix. When P_1B/GO composite was observed with 30,000 magnifications under 1 μm scale, it could clear to observe the surface of cured composites was relatively homogeneous. The improvement of these performance demonstrated that GO dispersed in the P_1B and P_2B polymer matrix very well. The homogeneous dispersion of GO is ascribed to the possible chemical grafting between the

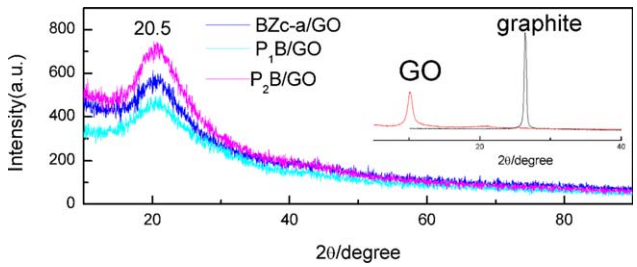

Figure 12. XRD spectra of BZc-a/GO, P_1B/GO, and P_2B/GO composites after curing. [Color figure can be viewed in the online issue, which is available at wileyonlinelibrary.com.]

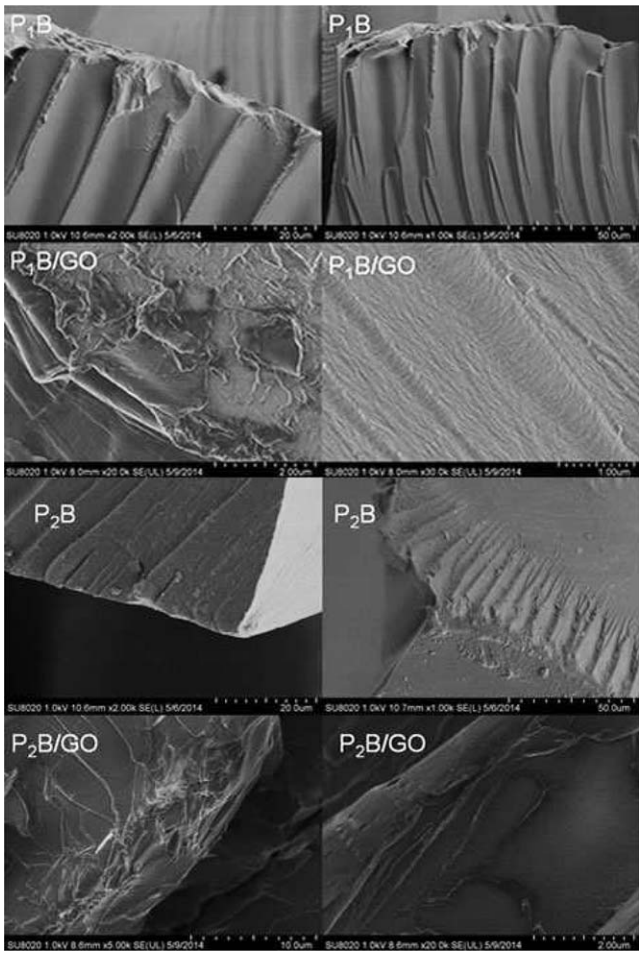

Figure 13. FESEM photographs of fracture surface of P_1B, P_1B/GO-3 wt %, P_2B, P_2B/GO-3 wt %.

O-containing groups of GO and the functional groups of prepolymer and generated P_1B-GO and P_2B-GO hybrid product, which enhanced the interfacial interaction of GO with P_1B and P_2B polymer matrix.

CONCLUSIONS

The different amount of DOPO reacted with a benzoxazine monomer based on cardanol were described in this article. Two containing phosphaphenanthrene compounds P_1B and P_2B were designed according to the structure characterizes of benzoxazine. The results obtained from fire test and TGA which all demonstrated that the addition of DOPO increased the thermal stabilities of benzoxazine. These two kinds of phosphorus compounds had well efficient on flame retardance. The presence of GO in P_1B and P_2B further improved their performance as materials. P_1B and P_2B could be used in resin as the chemical flame retardant additive. This work will be continued in future.

ACKNOWLEDGMENTS

This research receives financial supports from the National Natural Science Foundation of China (grant No. 51273054), and kindly supported by Key Laboratory of Biomimetic Sensor and Detection

Technology of AnHui, Lu'an in China and Engineering Technology Center of Fine Chemicals Engineering of AnHui, Lu'an in China.

REFERENCES

1. Ghosh, N. N.; Kiskan, B.; Yagci, Y. *Prog. Polym. Sci.* **2007**, *32*, 1344.
2. Takeichi, T.; Kawauchi, T.; Agag, T. *Polym. J.* **2008**, *40*, 1121.
3. Nair, C. *Prog. Polym. Sci.* **2004**, *29*, 401.
4. Kiskan, B.; Ghosh, N. N.; Yagci, Y. *Polym. Int.* **2011**, *60*, 167.
5. Kandaz, M.; Yılmaz, I.; Bekaroglu, O. *Polyhedron* **2000**, 115.
6. Brunovska, Z.; Lyon, R.; Ishida, H. *Thermochim. Acta* **2000**, 195.
7. Kim, S. G.; Kim, J.-H.; Yim, J.-H. *Macromol. Res.* **2013**, *21*, 1226.
8. Perret, B.; Schartel, B.; Stöß, K.; Ciesielski, M.; Diederichs, J.; Döring, M.; Krämer, J.; Altstädt, V. *Eur. Polym. J.* **2011**, *47*, 1081.
9. Siao, Y.-Y.; Shau, S.-M.; Hu, S.-H.; Lee, R.-H.; Lin, C.-H.; Wu, J.-Y.; Jeng, R.-*J. Polymer* **2013**, *54*, 3850.
10. Qian, X.; Song, L.; Yu, B.; Wang, B.; Yuan, B.; Shi, Y.; Hu, Y.; Yuen, R. K. K. *J. Mater. Chem. A* **2013**, *1*, 6822.
11. Hwang, H.-J.; Lin, C.-Y.; Wang, C.-S. *J. Appl. Polym. Sci.* **2008**, *110*, 2413.
12. Liu, Y. L. *Polymer* **2001**, 3445.
13. Liao, S.-H.; Liu, P.-L.; Hsiao, M.-C.; Teng, C.-C.; Wang, C.-A.; Ger, M.-D.; Chiang, C.-L. *Ind. Eng. Chem. Res.* **2012**, *51*, 4573.
14. Schartel, B. *Materials* **2010**, *3*, 4710.
15. Ling, H. G.; Ye, Z. I. A.; Gu, Y. I. *Polym. Mater. Sci. Eng.* **2010**, *26*, 86.
16. Lin, C. H.; Lin, H. T.; Sie, J. W.; Hwang, K. Y.; Tu, A. P. *J. Polym. Sci. Polym. Chem.* **2010**, *48*, 4555.
17. Xu, M. Z. *Express Polym. Lett.* **2013**, *7*, 984.
18. Rao, B. S.; Palanisamy, A. *Eur. Polym. J.* **2013**, *49*, 2365.
19. Xu, G.-M.; Shi, T.; Liu, J.; Wang, Q. *J. Appl. Polym. Sci.* **2014**, 131.
20. Marcano, D. C.; Kosynkin, D. V.; Berlin, J. M.; Sinitskii, A.; Sun, Z.; Slesarev, A.; Alemany, L. B.; Lu, W.; Tour, J. M. *ACS Nano* **2010**, *4*, 4806.
21. Wang, Y.; Shi, Z.; Fang, J.; Xu, H.; Yin, J. *Carbon* **2011**, *49*, 1199.
22. Ho, K.-K.; Hsiao, M.-C.; Chou, T.-Y.; Ma, C.-C. M.; Xie, X.-F.; Chiang, J.-C.; Yang, S.-H.; Chang, L.-H. *Polym. Int.* **2013**, *62*, 966.
23. Chang, H. C.; Lin, H. T.; Lin, C. H. *Polym. Chem.* **2012**, *3*, 970.
24. Zúñiga, C.; Larrechi, M. S.; Lligadas, G.; Ronda, J. C.; Galià, M.; Cádiz, V. *Polym. Degrad. Stab.* **2013**, *98*, 2617.
25. Huang, G.; Gao, J.; Wang, X.; Liang, H.; Ge, C. *Mater. Lett.* **2012**, *66*, 187.
26. Zúñiga, C.; Lligadas, G.; Ronda, J. C.; Galià, M.; Cádiz, V. *Polymer* **2012**, *53*, 3089.
27. Su, H.; Liu, Z. *J. Therm. Anal. Calorim.* **2013**, *114*, 1207.
28. Wang, X.; Song, L.; Pornwannchai, W.; Hu, Y.; Kandola, B. *Compos. A Appl. S.* **2013**, *53*, 88.
29. Steurer, P.; Wissert, R.; Thomann, R.; Mülhaupt, R. *Macromol. Rapid Commun.* **2009**, *30*, 316.
30. Hu, H.; Wang, X.; Wang, J.; Liu, F.; Zhang, M.; Xu, C. *Appl. Surf. Sci.* **2011**, *257*, 2637.
31. Stankovich, S.; Piner, R. D.; Nguyen, S. T.; Ruoff, R. S. *Carbon* **2006**, *44*, 3342.
32. Deng, P.; Xu, Z.; Kuang, Y. *Food Chem.* **2014**, *157*, 490.
33. Garg, V.; Kumar, A.; Chaudhary, A.; Agrawal, S.; Tomar, P.; Sreenivasan, K. K. *Med. Chem. Res.* **2013**, *22*, 5256.
34. Wang, D.; Li, B.; Zhang, Y.; Lu, Z. *J. Appl. Polym. Sci.* **2013**, 516.
35. Zeng, M.; Wang, J.; Li, R.; Liu, J.; Chen, W.; Xu, Q.; Gu, Y. *Polymer* **2013**, *54*, 3107.